CrossMark

Unpinning spiral wave anchored to two obstacles

SHREYAS PUNACHA[1], M. ABHISHEK[1,2] and T. K. SHAJAHAN[1,*]

[1]Department of Physics, National Institute of Technology Karnataka, Surathkal 575 025, India
[2]Simons Centre for the Study of Living Machines, National Centre for Biological Sciences (TIFR), Bellary Road, Bengaluru 560 065, India
*Corresponding author. E-mail: shajahan@nitk.edu.in

Abstract. Excitation waves in two-dimensional media form various travelling wave patterns such as spiral and target waves. These waves can interact with heterogeneities in the tissue. Spiral waves can attach and form stable pinned waves in heterogeneous excitable media. These spirals can be unpinned by delivering a carefully timed electric stimulus, delivered very close to the core. We study the spiral wave unpinning when a wave is attached to two obstacles at the same time. We show that the unpinning window decreases as the distance between the obstacles increases, and beyond a critical distance, this window completely vanishes. Our study implies that the distribution of heterogeneities can play a critical role in developing the low-energy defibrillation methods.

1. Introduction

Rotating spiral waves are commonly found in physiological and biological media like cardiac tissue [1], human tongue [2], retinal tissues [3] and chemical reactions like the Belousov–Zhabotinsky (B–Z) reaction [4]. In the heart, rotating cardiac excitation wave is known to cause a fatal cardiac arrhythmia like ventricular tachycardia (VT) and ventricular fibrillation (VF). During tachycardia, cardiac excitation rotates in the tissue overriding the natural rhythm set by heart's pace making cells. During fibrillation, these rotating waves break up and form multiple wavelets, leading to irregular electrocardiogram (ECG) patterns. The irregular propagation of the excitation waves causes asynchronous and irregular contraction of muscles in the heart. VF is known to cause about 300,000 deaths every year in the USA alone [1].

The dynamics of spiral waves can be understood by studying a generic excitable medium. The elements of the excitable medium respond to the external stimulus with a characteristic excitation only when the stimulus is above a certain threshold strength. The resulting excitation can propagate through the medium, as in a forest fire front, because of the diffusion-like coupling between the excitable elements. After such a wave, a second stimulus cannot initiate another excitation for a certain duration, known as the refractory period. Owing to this refractory period, travelling wave fronts in excitable media annihilate each other when they collide as they cannot excite the refractory tails behind the colliding wave.

The most frequently used method to terminate ventricular arrhythmia is via high-voltage defibrillation. The high-voltage shock depolarizes the entire heart at once for a short period of time, pushing it into a refractory state and eliminating all the excitation at once. This often leads to tissue damage like scars and lesions in the heart tissue, which could become seed for further episodes of arrhythmia. It is, therefore, essential to find better low-energy methods to defibrillate the heart.

In a method called anti-tachycardia pacing (ATP), the low-intensity pulses are given far away from the spiral core. These pulses generate target waves emanating from the location of stimulus electrode. If the pacing frequency is higher than the frequency of the spiral, these target waves can push the spiral wave away from the medium [5]. The success rate of ATP is found to be 60–90% [6]. While they are able to remove the rotating spirals freely, in heterogeneous medium, excitation waves tend to form a stable rotating pattern around a heterogeneity in the medium. This is known as wave pinning. If not unpinned, these pinned spirals can rotate indefinitely [7]. It is therefore imperative to find optimal conditions and device efficient methods to unpin them.

To unpin the spiral pinned to an obstacle, the stimulus has to be applied in the refractory tail, close to the core of the spiral wave [8, 9]. This narrow time window, where the spiral unpins, is called the

unpinning window of the spiral. The stimulus delivered in this unpinning window will nucleate a wave, which can travel only in the direction opposite to the spiral due to the refractory property of the excitable media. Eventually, the wave nucleated by the stimulus and the spiral will collide head-on and annihilate each other, unpinning the spiral. To get the stimulus delivered to the core of the spiral wave, we use a technique called far field pacing (FFP) [10]. When a low-voltage global electric field is applied across a medium with obstacles, depolarization and hyperpolarization regions form on either side of the obstacles. These regions are called Weidmann zones [6]. Above a threshold value of the electric field, the depolarization region can nucleate an excitation wave. A stimulus is delivered in such a way that the wave it nucleates will fall into the unpinning window can unpin the spiral wave.

Unpinning of a wave attached to a single obstacle has been extensively studied using FFP by Takagi *et al.* [11], Pumir *et al.* [12] and Bittihn *et al.* [13]. The unpinning success using the velocity restitution effects in detailed cardiac models is studied by Isomura *et al.* [14]. The pinned spiral waves' response to the periodic stimuli is carried out in detail by Shajahan *et al.* [9] and Behrend *et al.* [15], where an alternative and robust approach to finding the pacing frequencies for unpinning is discussed.

In this paper, we study the effect of the unpinning window by introducing a second obstacle near the central obstacle. We study the special case of unpinning where the spiral tips are attached to both the obstacles. By delivering the low-voltage stimulus at different phases of the spiral and systematically changing the distance between the two obstacles, we try to understand the unpinning window of the two-obstacle system.

2. Methods

All the simulations in this paper are carried out using the Barkley [16] model, which is a modified Fitzhugh–Nagumo type model proposed by Dwight Barkley to simulate the cardiac action potential efficiently. The model equations are as follows:

$$\frac{\partial u}{\partial t} = \frac{1}{\epsilon} u(1-u)\left(u - \frac{v+b}{a}\right) + D\nabla^2 u, \quad \frac{\partial v}{\partial t} = u - v. \quad (1)$$

Here, u represents the dimensionless transmembrane potential whereas v stands for all the time-dependent gating variables. For simplicity, in modelling, v is assumed to be not to diffuse. The variable u is responsible for the excitation process and v is the slow inhibitory variable, accountable for refractory period of the medium following the excitation. The parameter ϵ

determines how fast u changes with respect to v. The parameter a controls the width of the action potential and b/a determines the threshold of excitation. The parameters are set to $a = 0.53$, $b = 0.05$ and $\epsilon = 0.02$ throughout the simulations.

The Barkley model equations are solved in a 300×300 computational grid using the forward Euler method. A five-point stencil is used to compute the Laplacian. Neumann boundary conditions are implemented at the domain boundaries to ensure that no flux escapes from the boundary. The computation is carried out using a spatial resolution $dx = 0.1$ and the Euler time step $dt = 0.001$. The accuracy of the Euler scheme has been tested systematically for smaller spacial resolutions ($dx = 0.05, 0.01$) and the quantities such as action potential duration and wavelength of the spiral are found to agree with each other. The electric field is applied using the no-flux boundary conditions [6], as given below:

$$\hat{y} \cdot (D\nabla u - \vec{E}) = 0, \quad (2)$$

where $\hat{y}$ is a unit vector perpendicular to the obstacle boundary, D is the coupling constant and $\vec{E}$ is the applied electric field. The Neumann boundary conditions in eq. (2) can be implemented easily since the boundaries of the obstacle are parallel to the coordinate axis. In simulations, we apply the electric field along the y-axis. Then, eq. (2) becomes
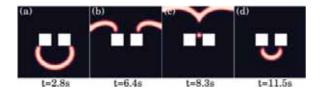
$$D\frac{\partial u}{\partial y} = E_y. \quad (3)$$

The strength of the electric field is set to $\vec{E} = 3$ units and the pulse duration is set to 0.5 s. All the distances are measured in terms of the wavelength ($\lambda = 48$) of the spiral. The wavelength of the spiral is the number of space steps between the wave front and the wave back.
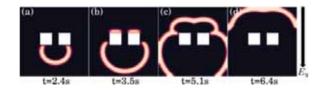
3. Results and discussion

To study the unpinning in the presence of multiple obstacles, we simulated a rotating wave attached to two obstacles in a medium, as shown in figures 1a–d. The wave rotates with a period of 10 s. In figure 1 the obstacles are at a distance of 0.625λ apart. We define the phase as the position of the spiral at the time of the pulse in one complete spiral period. So $\Phi \in [0, 1]$.

To determine the unpinning window of the above-mentioned spiral, we deliver a low-voltage electrical stimulus along the negative y-axis (as shown in figure 2a) at different phases of the spiral. After the application of the electric field, the secondary waves are nucleated at $t = 3.5$ s (figure 2b) due to the phenomenon of wave emission from heterogeneity (WEH) [8].

Figure 1. Spiral wave with its tip attached to both the obstacles. The obstacles are at a distance of 0.625λ apart, where λ is the wavelength of the spiral wave. We treat this spiral as our initial condition for all the simulations. (**a**) $t = 2.8$ s, (**b**) $t = 6.4$ s, (**c**) $t = 8.3$ s and (**d**) $t = 11.5$ s.
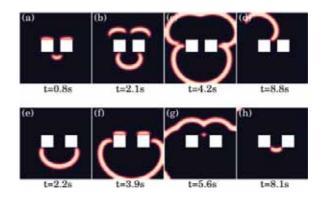

Figure 2. Successful unpinning of the spiral wave attached to both the obstacles. The FFP stimulus makes the obstacles emit secondary excitations at $t = 3.5$ s. The tips of the secondary excitation and the spiral wave meet at $t = 5.1$ s which result in their annihilation. The wave is unpinned and moves away from the boundary, as shown at $t = 6.4$ s. (**a**) $t = 2.4$ s, (**b**) $t = 3.5$ s, (**c**) $t = 5.1$ s and (**d**) $t = 6.4$ s.

Figure 3. Cases of unsuccessful unpinning. In figures (**a**)–(**d**) the spiral tips on the left do not collide with each other perfectly. Due to imperfect collision wave, which survives in the medium later, develops into a pinned spiral as shown in figure (**d**). In figures (**e**)–(**h**) the distance between the obstacles has been increased to 1.014λ. This allows the secondary excitations from the obstacles to develop more curvature which results in the incomplete unpinning. The resulting wave will be attached to both the obstacles as shown in figure (**h**). (**a**) $t = 0.8$ s, (**b**) $t = 2.1$ s, (**c**) $t = 4.2$ s and (**d**) $t = 8.8$ s, (**e**) $t = 2.2$ s, (**f**) $t = 3.9$ s, (**g**) $t = 5.6$ s and (**h**) $t = 8.1$ s.

The emitted wave will then successfully unpin the spiral wave, as shown in figures 2c and d.

The unpinning shown in figure 2 is unique because the secondary excitation is not nucleated in the refractory tail of the spiral. Instead, the secondary excitation is nucleated from top of the two obstacles. After the wave nucleation, there are four tips in total. The tips of the secondary excitation close to the spiral tips will collide and annihilate each other. The remaining two tips of the secondary excitation will also collide with each other at $t = 5.1$ s and move away from the obstacles, unpinning the spiral.

The unpinning mechanism mentioned above happens only in the small region in the phase window of the spiral. We call it the unpinning window of the two-obstacle system. But, if the spiral tips and the tips of the secondary excitation do not meet exactly, then they do not annihilate completely. This leaves a portion of the wave, which later develops and ends up pinning to one or either of the obstacles. The snapshots of failed unpinning due to the above-mentioned reason are shown in figures 3a–d.

In figures 3e–h, we show another case where the spiral fails to unpin from the obstacle. Here, the distance between the obstacles is increased to 1.014λ. As the distance between the obstacles increases, the tips generated from the secondary excitations will continue to collide and annihilate with the tips of the spiral wave. However, the tips of the secondary excitations will have to move a larger distance before they collide and
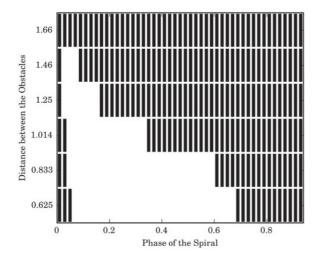
annihilate. The increase in distance will give more time to develop curvature, so that their tips do not coincide with each other exactly. The wave left out due to inefficient collision will be developed into a new pinned spiral wave, as shown in figure 3h.

The above-mentioned unpinning mechanism shows that the spiral wave, which is attached to both the obstacles, does not have a conventional unpinning window, but it does have an unpinning window of its own. We plot a graph that indicates the unpinning window as a function of distance between the obstacles corresponding to the electric field stimulus being applied at different phases of the spiral. From the graph, we see that at lower distances between the obstacles, we observe a large unpinning window. This success in unpinning can be attributed to the mechanism explained in figure 2. The unpinning window decreases as the distance between the obstacles increases (see figure 4). This is because of the unsuccessful cases mentioned in figure 3. After a certain distance $d = 1.46\lambda$ the window vanishes completely.

4. Conclusions

In this paper, we have discussed the wave unpinning from two obstacles. We have shown that the chances of unpinning, as quantified by the unpinning window, decreases as the distance between the obstacles increases. After a critical distance, unpinning fails completely. Our results show that to unpin a spiral anchored to both the obstacles, it is not essential for

Figure 4. Unpinning window of the two-obstacle system. White coloured grids indicate unpinning and black grids indicate failed unpinning. Distance between the obstacles is measured in terms of spiral wavelength. The stimulus is given for every 0.2 s for six different distances. From the graph, it is clear that the unpinning window decreases as the distance between the obstacles increases.

the stimulus, which is delivered, to fall into the refractory tail of the spiral. It is sufficient if the tips of the secondary excitation will annihilate with the tips of the spiral wave.

Our results will be relevant in deciding the FFP-based methods for low-energy fibrillation. In particular, the distribution of heterogeneities can play a critical role in deciding the unpinning window. The length of the unpinning window can be altered by the presence of neighboring heterogeneities.

Acknowledgement

References

[1] A Karma, *Annu. Rev. Condens. Matter Phys.* **4(1)**, 313 (2013)

[2] G Seiden and S Curland, *New J. Phys.* **17(3)**, 033049 (2015)

[3] X Huang, W C Troy, Q Yang, H Ma, C R Laing, S J Schiff and J-Y Wu, *J. Neurosci.* **24(44)**, 9897 (2004)

[4] W Jahnke, W Skaggs and A T Winfree, *J. Phys. Chem.* **93(2)**, 740 (1989)

[5] C M Ripplinger, V I Krinsky, V P Nikolski and I R Efimov, *Am. J. Physiol.-Heart Circul. Physiol.* **291(1)**, H184 (2006)

[6] A Pumir and V Krinsky, *J. Theor. Biol.* **199(3)**, 311 (1999)

[7] S Luther *et al.*, *Nature* **475(7355)**, 235 (2011)

[8] P Bittihn, M Hörning and S Luther, *Phys. Rev. Lett.* **109(11)**, 118106 (2012)

[9] T Shajahan, S Berg, S Luther, V Krinski and P Bittihn, *New J. Phys.* **18(4)**, 043012 (2016)

[10] P Bittihn, G Luther, E Bodenschatz, V Krinsky, U Parlitz and S Luther, *New J. Phys.* **10(10)**, 103012 (2008)

[11] S Takagi, A Pumir, D Pazó, I Efimov, V Nikolski and V Krinsky, *J. Theor. Biol.* **230(4)**, 489 (2004)

[12] A Pumir, V Nikolski, M Hörning, A Isomura, K Agladze, K Yoshikawa, R Gilmour, E Bodenschatz and V Krinsky, *Phys. Rev. Lett.* **99(20)**, 208101 (2007)

[13] P Bittihn, A Squires, G Luther, E Bodenschatz, V Krinsky, U Parlitz and S Luther, *Philos. Trans. A Math. Phys. Eng. Sci.* **368(1918)**, 2221 (2010)

[14] A Isomura, M Hörning, K Agladze and K Yoshikawa, *Phys. Rev. E* **78(6)**, 066216 (2008)

[15] A Behrend, P Bittihn and S Luther, *IEEE Computing in Cardiology* (Belfast, UK, 26–29 September, 2010), pp. 345–348

[16] D Barkley, *Physica D* **49(1–2)**, 61 (1991)